



Cite this: DOI: 10.1039/c7an00970d

A surface plasmon field-enhanced fluorescence reversible split aptamer biosensor†

K. Sergelen,^{a,b,c} B. Liedberg,^b W. Knoll^a and J. Dostálek^{b,*a}

Surface plasmon field-enhanced fluorescence is reported for the readout of a heterogeneous assay that utilizes low affinity split aptamer ligands. Weak affinity ligands that reversibly interact with target analytes hold potential for facile implementation in continuous monitoring biosensor systems. This functionality is not possible without the regeneration of more commonly used assays relying on high affinity ligands and end-point measurement. In fluorescence-based sensors, the use of low affinity ligands allows avoiding this step but it imposes a challenge associated with the weak optical response to the specific capture of the target analyte which is also often masked by a strong background. The coupling of fluorophore labels with a confined field of surface plasmons is reported for strong amplification of the fluorescence signal emitted from the sensor surface and its efficient discrimination from the background. This optical scheme is demonstrated for time-resolved analysis of chosen model analytes – adenoside and adenosine triphosphate – with a split aptamer that exhibits an equilibrium affinity binding constant between 0.73 and 1.35 mM. The developed biosensor enables rapid and specific discrimination of target analyte concentration changes from low μM to mM in buffer as well as in 10% serum.

Received 10th June 2017,
Accepted 6th July 2017

DOI: 10.1039/c7an00970d

rscl.li/analyst

Introduction

In recent years, a rapidly increasing number of analytical technologies have taken advantage of cost-effective production and flexibility in the design of oligonucleic acid aptamer ligands.^{1–3} Among others, aptamer biosensors found their applications in sensitive analysis of species that serve as biomarkers of cancer,^{4–6} cardiovascular diseases,^{7,8} and inflammation^{9–11} as well as for the detection of pathogens.^{3,12,13} The optical readout of the specific interaction of an aptamer ligand with a target analyte mostly utilizes fluorescence.^{14–16} The majority of fluorescence-based aptamer biosensors rely on distance-dependent fluorescence resonance energy transfer (FRET)^{17,18} or quenching of the fluorescence signal in the vicinity of graphene^{13,19,20} and other quenchers.^{21,22} The performance of fluorescence-based biosensors is

often limited by the background signal and bleaching of fluorophore labels. This problem may be overcome by the use of surface plasmon resonance (SPR) biosensors which provide a facile platform for the direct detection of a target analyte that does not require labels.^{23–25} SPR aptamer biosensors exploiting localized surface plasmons supported by metallic nanoparticles^{12,26,27} and propagating surface plasmons travelling along thin metallic films¹¹ were reported. Moreover, surface plasmon optics can be employed for the amplification of the fluorescence assay readout by probing of aptamer binding with plasmonically enhanced intensity of the electromagnetic field. This phenomenon was exploited with the use of propagating surface plasmons on metallic surfaces^{28–31} as well as with localized surface plasmons supported by metallic nanoparticles spiked to the analyzed liquid sample.^{32,33} Besides the plasmon-enhanced fluorescence (PEF) intensity, this detection scheme typically decreases the lifetime of the used fluorophore labels which reduces the effect of bleaching.^{34,35}

The sandwich format is routinely used in immunoassays for the detection of medium and large molecular weight analytes. In this method, one antibody is attached to a sensor surface to capture the target analyte from the analyzed sample. Subsequently, the surface is reacted with the second antibody that is labeled with a reporter (e.g. fluorophore or nanoparticle).³⁶ These two antibodies are designed so that they bind to different epitopes of the target analyte without steric hindrance. This approach is generally not possible for low

^aBioSensor Technologies, AIT-Austrian Institute of Technology, Muthgasse 11, 1190 Vienna, Austria. E-mail: jakub.dostalek@ait.ac.at; Fax: +43 50550-4450; Tel: +43 50550 4470

^bNanyang Technological University, Centre for Biomimetic Sensor Science, School of Materials Science and Engineering, 50 Nanyang Drive, Singapore 637553

^cInternational Graduate School on Bionanotechnology, University of Natural Resources and Life Sciences, Austrian Institute of Technology (Austria) and Nanyang Technological University (Singapore)

† Electronic supplementary information (ESI) available: Surface mass density values of the functionalized sensor chip and fitted calibration curves of each of the target analytes with determined dissociation constants. See DOI: 10.1039/c7an00970d

molecular weight analytes. Aptamers on the other hand provide an interesting alternative to established immunoassays and they are particularly attractive for rapid detection of low molecular-weight analytes.^{10,17,18,26} Single strand oligonucleotide aptamers were also implemented in biosensors utilizing a sandwich assay.^{37–39} In contrast to immunoassays, they offer means to design sandwich-type assays even for low molecular weight analytes^{40–44} by using an aptamer sequence divided into two separate strands in a way that allows maintaining the binding activity.

The sandwich aptamer assay was utilized for continuous sensing of biologically active analytes⁴⁵ which was reported for time-resolved measurements of species secreted by cells to their local environment. Indeed, the vast majority of biosensors rely on high affinity ligands. Then regeneration protocols need to be applied to strip the captured analyte from the ligand for their repeated use.^{46,47} However, such regeneration complicates the operation in emerging applications such as cell-on-chip⁴⁸ or therapeutic drug monitoring.⁴⁹ In principle, more facile monitoring of time dependent analyte concentration variations can be utilized by low affinity ligands.^{50–53} In sandwich aptamer assays that utilize SPR metallic nanoparticles as reporters, usually multiple aptamer (oligonucleotide) strands are attached which often leads to avidity-enhanced irreversible interactions with the analyte. This can be overcome by tedious purification steps⁴⁵ or with the use of fluorophore tags that do not increase affinity.⁵⁴

The use of weak affinity ligands for reversible fluorescence-based sandwich assaying is challenging due to the high fluorescence background and weak specific signals associated with the analyte capture. We report herein the implementation of PEF as a sensitive readout method for reversible split aptamer-based fluorescence biosensing. A split DNA aptamer^{55,56} that binds to ATP and adenosine was chosen for a proof of concept demonstration of real-time continuous monitoring of concentration changes without the need of regeneration.

Experimental

Materials

Adenosine 5'-triphosphate disodium salt hydrate (ATP), adenosine, guanosine, sodium chloride, magnesium chloride hexahydrate, tris hydrochloride, 4-(2-hydroxyethyl)piperazine-1-ethanesulfonic acid (HEPES) and polyethylene glycol sorbitan monolaurate (TWEEN 20) were obtained from Sigma-Aldrich (Austria). Neutravidin protein was purchased from ThermoFisher (Austria). Biotinylated alkane PEG thiol (BA thiol, SPT-0012D) and (11-mercaptoundecyl) triethyleneglycol (PEG thiol, SPT-0011) were purchased from SensoPath Technologies Inc. (USA). Buffer solutions were prepared using ultrapure water (arium pro, Sartorius Stedim) with all reagents used as received. The ATP and adenosine binding split DNA aptamer⁵⁵ sequences Biotin 5'-TTTTTTTTTTTAGA GAA CCT GGG GGA GTA T-3' (segment S1-Biotin) and AlexaFluor647N 5'-TTTTTTGC GGA GGA AGG TAG AG-3' (segment S2-AF647) were synthesized by Integrated DNA Technologies (Belgium). The

serum sample was collected from a healthy donor using a Vacuette Z Serum Clot Activator (Freiner Bio One, Germany), centrifuged for 10 minutes at 1800g and stored at -20°C until analysis.

Sensor chip preparation

Sensor chips were prepared on BK7 glass substrates which were subsequently coated with 2 nm chromium and 50 nm gold films by thermal vacuum evaporation (HHV Auto306 Lab Coater). The thickness of gold was chosen to maximize the coupling strength to propagating surface plasmons based on previous work reported in the literature.⁵⁷ The gold surfaces were rinsed with ethanol, dried under a stream of air and immersed in 1 mM ethanolic solution with BA and PEG thiols dissolved at a 1:9 ratio. This ratio was reported as optimum for the immobilization of oligonucleotide strands by streptavidin–biotin interactions.⁵⁸ After 48 hours of incubation under an argon atmosphere, a mixed self-assembled monolayer (SAM) was formed on the gold surface which was subsequently rinsed with ethanol and dried under a stream of air. A 10 mM HEPES buffer (pH = 7.4) containing 150 mM NaCl, 5 mM MgCl_2 and 0.005% Tween 20 was used throughout the immobilization of the ligand. Initially, 0.5 mL of $50\ \mu\text{g mL}^{-1}$ neutravidin solution was flowed over the mixed thiol SAM for 25 minutes to form a monolayer.⁵⁷ Then, 0.5 mL of $1\ \mu\text{M}$ solution of biotinylated split aptamer segment 1 (S1-Biotin) was reacted with the surface for 25 minutes in which the saturation was reached. After each incubation step, the sensor surface was rinsed for 10 minutes with buffer.

Optical measurements

For the optical measurements, an instrument that combines surface plasmon resonance (SPR) and surface plasmon field-enhanced fluorescence (PEF) was used as described previously.⁵⁹ Briefly, the sensor chip with the mixed thiol SAM was optically matched to an LASFN9 glass prism with refractive index matching oil (Cargille Inc., USA) and a flow-cell was clamped onto its top. The volume of the flow-cell was $10\ \mu\text{L}$ and it consisted of a PDMS gasket (thickness of $\sim 130\ \mu\text{m}$) and a transparent glass substrate with drilled inlet and outlet ports. Liquid samples were transported *via* a tubing (Tygon LMT-55) with a 0.25 mm inner diameter at a flow rate of $15\ \mu\text{L min}^{-1}$. This assembly was mounted onto a rotating stage and a monochromatic transverse magnetically (TM) polarized HeNe laser ($\lambda_{\text{ex}} = 632.8\ \text{nm}$) beam was coupled to the prism. The angle of incidence θ was controlled to resonantly excite the propagating surface plasmons (PSPs) on the gold surface by the Kretschmann configuration of the attenuated total reflection method. The reflected light intensity R was measured by using a photodiode detector connected to a lock-in amplifier (EG&G, USA). In addition, the fluorescence intensity F emitted at wavelength $\lambda_{\text{em}} = 670\ \text{nm}$ through the flow-cell in the direction normal to the gold surface was collected with a lens (focal length 30 mm, numerical aperture NA = 0.2). Two bandpass filters (transmission wavelength $\lambda_{\text{em}} = 670\ \text{nm}$, 670FS10-25, Andover Corporation Optical Filter, USA) and a notch filter

(central stop-band wavelength $\lambda_{\text{ex}} = 632.8$ nm, XNF-632.8-25.0 M, CVI Melles Griot, USA) were used to block the excitation light at λ_{ex} . Afterwards, the beam at λ_{em} was coupled to a multi-mode optical fiber (FT400EMT, Thorlabs, UK) and detected with an avalanche photodiode (Count-200-FC, Laser Components, Germany). The fluorescence light intensity F was measured using a counter (53131A, Agilent, USA) in counts per second (cps). Both the reflectivity and fluorescence signals were recorded using the software Wasplas (Max Planck Institute for Polymer Research, Mainz, Germany). Time resolved measurements of reflectivity R and fluorescence intensity F were performed at a fixed incidence angle θ .

Split aptamer assay

In the split aptamer assay, the HEPES buffer solution with 100 nM S2-AF647 aptamer (concentration derived from data shown in Fig. S2†) was continuously flowed over the sensor surface with immobilized aptamer S1-Biotin. After establishing a stable baseline in the acquired fluorescence signal F_0 in about 15 minutes, sequential analysis of samples with the target (ATP, adenosine) and reference (guanosine) analytes was performed. These analytes were spiked into the buffer with 100 nM S2-AF647 and each sample was allowed to react with the surface for 5–8 minutes until a steady level of fluorescence signal $F(t)$ was reached.

Results and discussion

Surface plasmon field-enhanced fluorescence split aptamer assay

As can be seen in Fig. 1, the used split aptamer ligand is composed of two segments. The segment S1-Biotin was immobi-

lized on the sensor surface by using the biotin tag, while the second segment S2-AF647 carrying Alexa Fluor 647 label was contained in a solution above the surface. Split aptamer sequences that specifically bind to adenosine and ATP were adopted from studies reported in the literature.^{55,56} In the presence of the target analyte, the segment S2-AF647 forms a complex with tethered S1-Biotin, whereas in the absence of the target analyte the segments do not interact. The S2-AF647 binding events triggered by the presence of the target analyte were monitored by probing of the gold sensor surface with resonantly excited surface plasmons – PSPs. The excitation of PSPs generates an increased intensity of electromagnetic field at a wavelength of $\lambda_{\text{ex}} = 633$ nm which coincides with the absorption band of the used fluorophore. Due to its confined field profile, the PSP-enhanced excitation of fluorophores occurs only in the close proximity of the sensor surface (below <100 nm). The fluorescence light intensity F that was emitted perpendicularly to the surface at a wavelength of $\lambda_{\text{em}} = 670$ nm was collected and detected in time.

The intensity of the emitted fluorescence signal is strongly dependent on the distance of the fluorophore from the gold surface.²⁹ In order to prevent quenching occurring at short distances of <10 nm, surface architecture with a neutravidin spacer layer was used for the immobilization of the S1-Biotin segment. Then the affinity binding occurs further away from the gold and the effect of quenching is substantially reduced as reported previously for the surface plasmon-enhanced fluorescence detection of DNA hybridization.⁶⁰

Aqueous samples with varying concentrations of ATP were prepared. Each sample was spiked with the same concentration of aptamer segment S2-AF647 of 100 nM and flowed over the sensor surface for 5–8 min. Upon the flow of samples, a series of fluorescence intensity scans $F(\theta)$ were measured for different angles of incidence θ of the excitation laser beam at λ_{ex} . As shown in Fig. 2, strong fluorescence intensity F was

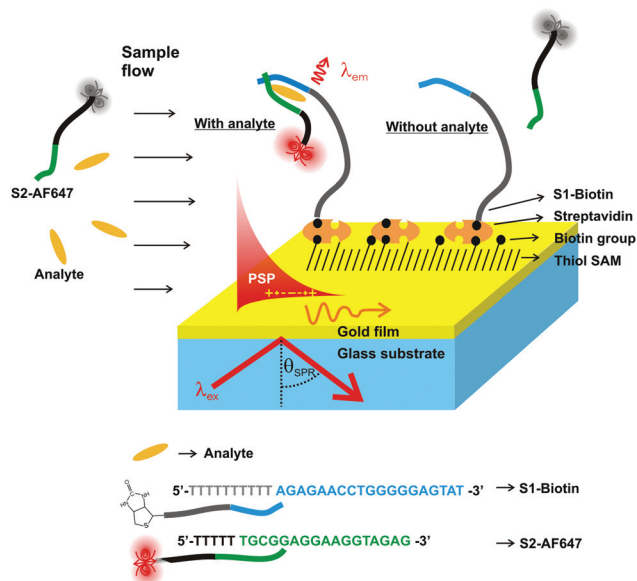


Fig. 1 Schematics of the split aptamer sandwich assay and surface architecture.

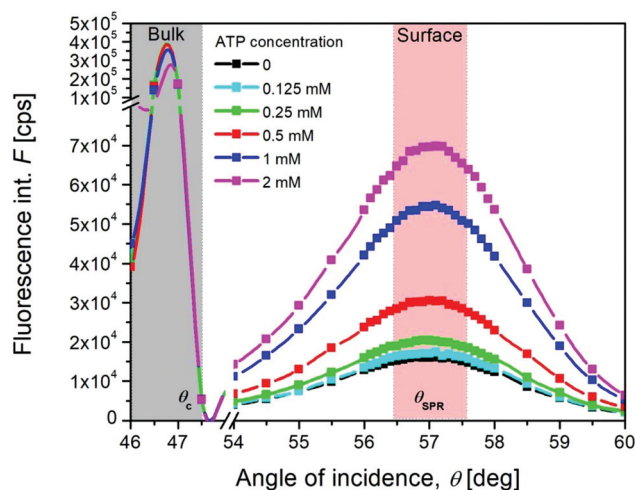


Fig. 2 Angular fluorescence intensity spectra $F(\theta)$ measured upon the affinity binding of ATP to the sensor surface from samples with ATP concentration from 0.125 to 2 mM.

observed at angles θ below the critical angle ($\theta_c = 47.3$ deg). This fluorescence signal originates from fluorophores dispersed in the bulk solution that are excited with a laser beam partially transmitted through the gold layer. When increasing the angle θ above the critical angle θ_c , the fluorescence signal F drops and an additional fluorescence peak is observed at a higher angle $\theta_{\text{SPR}} \sim 57$ deg. This peak is ascribed to the fluorescence signal emitted from the surface when PSPs are resonantly excited at λ_{ex} . Interestingly, when increasing the concentration of ATP in the solution, the fluorescence signal below the critical angle θ_c does not significantly change. In contrast, probing of the sensor surface with the confined field of PSPs at angle θ_{SPR} is accompanied by fluorescence intensity that increases with ATP concentration. The reason is that below the critical angle θ_c the measured fluorescence signal F mostly originates from the fluorophore labeled segment of the aptamer S2-AF647 that is contained in the bulk solution. This signal apparently masks the response due to the affinity binding on the sensor surface. However, above the critical angle θ_c the fluorescence excitation *via* the enhanced intensity of the evanescent PSP field occurs. Such optical enhancement is selective for the surface and efficiently makes the affinity binding of the target analyte distinguishable from the bulk. The simultaneously measured angular reflectivity spectra $R(\theta)$ (Fig. S3†) reveal no measurable shift in the SPR angle (represented as a minimum of the respective reflectivity dip) as the local refractive index variations associated with low molecular weight analyte binding are too weak.

Time-resolved fluorescence readout

In order to measure the fluorescence response upon the affinity binding of the target analyte in time, the angle of incidence was fixed at $\theta = 57$ deg where the strongest fluorescence enhancement was observed. Firstly, a steady baseline in the fluorescence signal F_0 was established for a flow of a blank sample with 100 nM S2-AF647. Then, a series of samples

spiked with the target analytes (ATP or adenosine) and the reference analyte (guanosine) were sequentially injected. Increasing the concentration of adenosine leads to a gradual increase of the fluorescence signal F which saturates in about 5–8 min (see Fig. 3, left). For the highest injected ATP concentration of 2 mM, the equilibrium fluorescence signal F increased by a factor of ~ 4 with respect to the baseline F_0 . For the ATP concentrations above 2 mM, the fluorescence signal reached saturation. Compared to ATP, the binding of adenosine showed a stronger response and for the concentration of 5 mM the fluorescence signal increased by a factor of ~ 22 with respect to F_0 , reaching saturation. This observation can be ascribed to differences in the interaction of ATP and adenosine with the split DNA aptamer. Possibly the weaker association of ATP with the aptamer complex than that of adenosine can be attributed to the strong negative charges of both ATP and the fluorophore AF647 conjugated split aptamer segment S2-AF647. The reference analyte guanosine did not interact with the selected aptamer.

Importantly, the interaction of the split aptamer with the target analytes is fully reversible. When switching the flow of samples to a blank buffer sample with the same concentration of S2-AF647, but without the target analyte, the fluorescence signal quickly drops to the original baseline F_0 in 1 minute. The right panel in Fig. 3 confirms the full reversibility of the assay and demonstrates the potential for real-time continuous sensing by running several cycles of injection of the sample series with increasing ATP concentration. In the context of applying such a sensor for therapeutic drug monitoring, there would be a need to reach time resolution that is comparable to the drug half-life (mostly hours to days) or time to reach the peak concentration of the drug (30 min to >hours).^{61–64} The presented assay offers a much faster response as the sensor signal reaches equilibrium in several minutes after a change of the target analyte concentration. Indeed, it should be mentioned that the response time is probably dictated by diffusion

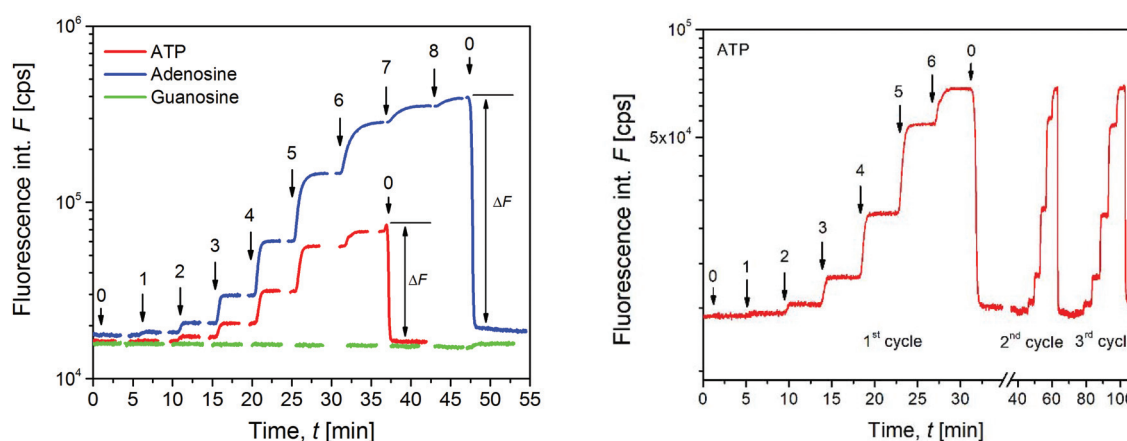


Fig. 3 The titration measurements illustrating the reversibility of the split aptamer based assay. Left. The red and blue lines indicate the specific analytes ATP and adenosine, respectively, and guanosine as the negative control (green line). Right. Demonstration of the reversible and reproducible detection of the assay for 3 rounds of ATP detection. Concentrations of analytes are indicated in sequential numbers: 0 – 0; 1 – 0.062 mM; 2 – 0.125 mM; 3 – 0.25 mM; 4 – 0.5 mM; 5 – 1 mM; 6 – 2 mM; 7 – 3 mM; 8 – 5 mM, respectively.

of the analyte to the surface and mixing of solutions in the used flow injection.

Calibration curves

From the titration experiments presented in Fig. 3, the equilibrium response was determined for each concentration as the difference of equilibrium signals $\Delta F = F - F_0$. The established calibration curves for ATP and adenosine are presented in Fig. 4 together with a fit using the Langmuir isotherm. From these data, the equilibrium dissociation constant K_d for the affinity interaction of ATP and adenosine with the split aptamer was determined. This parameter was obtained as the half saturation concentration and it yields a K_d of 0.35 mM and 1.35 mM for ATP and adenosine, respectively (Fig. S4†). It is worth noting that these values are in the range proposed for reversible continuous sensing, $K_d > \mu\text{M}$.⁵⁰ In addition, they are about two orders of magnitude higher than those for the affinity interaction with the native (not split) aptamer in the bulk solution, $K_d \sim 6 \mu\text{M}$.⁵⁶ The weaker affinity with respect to the reported heterogeneous assay can be partially attributed to the labeling of aptamer strands with fluorophores which was observed before ($K_d = 273 \mu\text{M}$ ⁵⁴).

The limit of detection for the assay was determined for each calibration curve as the concentration at which the value of 3 times the standard deviation of the background signal F_0 ($3\sigma = 2.5\%$ of F_0 for ATP and $3\sigma = 2\%$ of F_0 for adenosine) intersects with the fitted calibration curve. The LOD values of $78 \mu\text{M}$ and $42 \mu\text{M}$ were determined for ATP and adenosine, respectively. Such a detection limit is not sufficient for the analysis of ATP or adenosine as a biomarker in clinical samples such as plasma⁶⁵ or extracellular space⁶⁶ where they are present at concentrations in the low nM range. However, it may be feasible to apply a similar split aptamer for the sensing

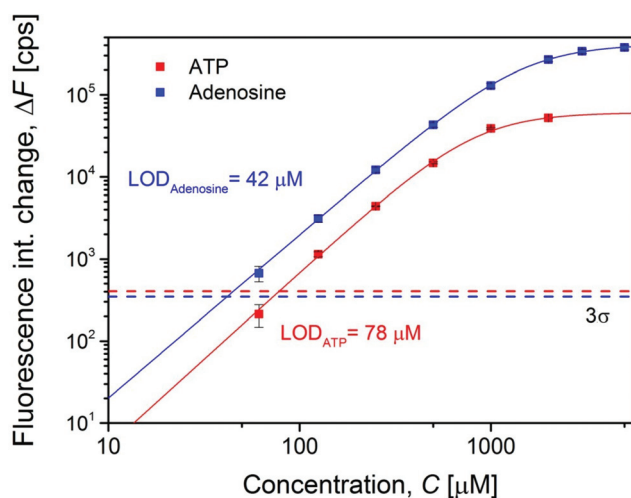


Fig. 4 Calibration curves of the detection of ATP and adenosine analytes. Each data point (ΔF) is derived from triplicate titration measurements as in Fig. 3. Calibration curves were fitted with the Langmuir isotherm model.

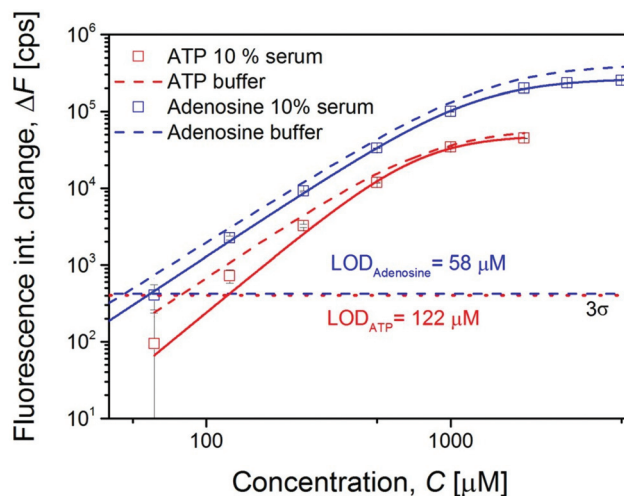


Fig. 5 Comparison of the calibration curves of ATP and adenosine detection measurements in buffer and 10% serum.

of the cellular sub mM levels of ATP⁶⁷ in cell-on-chip systems that are combined with fluorescence microscopy.⁶⁸ Plasmonic amplification of the fluorescence signal in such a detection scheme can be implemented with the use of an epifluorescence readout as reported before by our group.²⁸ In addition, the limit of detection can be improved by using more powerful plasmonic amplification schemes⁶⁹ and by using biointerfaces that accommodate higher amounts of ligands such as those relying on 3D hydrogel matrices.⁷⁰ Moreover, depending on the needed time resolution in the monitoring of target analyte concentration changes, the implementation of ligands with higher affinity would directly translate to an improved LOD.

Assay performance in real samples

Finally, the performed split aptamer assay was tested for the analyte spiked into 10% serum with the same concentration ranges as used for sensing in buffer. Detection was performed in triplicate and from the obtained calibration curves, the LOD of the sensor in 10% serum is slightly increased to $122 \mu\text{M}$ for ATP and $58 \mu\text{M}$ for adenosine (Fig. 5). Although there is slight loss in the LOD of the reported assay in diluted serum, the reversible detection of analytes is retained (Fig. S5†) and the overall biosensor performance is comparable to that in buffer.

Conclusions

A DNA split aptamer assay with a surface plasmon field-enhanced fluorescence sensor was demonstrated to allow for reversible and label-free detection of small molecular weight analytes, ATP and adenosine. Real-time probing of the analyte/aptamer specific interaction with the spatially confined surface plasmon field enabled the efficient suppression of the effect of the fluorescence background. A fully reversible

aptamer biosensor with a detection limit in the low micromolar range was established. The applicability of the sensor scheme was proven for 10-fold diluted serum and the reversible detection of concentration changes of the analytes was possible in the time range of minutes. The reported reversible sensing scheme can pave a way for the future development of continuous optical sensors for the many medically relevant markers that require close monitoring, which is vital to the improved evaluation and treatment of patient states⁷¹ or it may find its application in lab-on-chip systems for the rapid monitoring of cellular constituents and metabolites over time.⁴⁸

Acknowledgements

K. S. acknowledges financial support from the Austrian Federal Ministry for Transport, Innovation and Technology (GZ BMVIT-612.166/0001-III/11/2010). J. D. received support from the Tan Chin Tuan foundation, College of Engineering, Nanyang Technological University.

References

- 1 S. Amaya-González, N. de-los-Santos-Álvarez, A. Miranda-Ordieres and M. Lobo-Castañón, *Sensors*, 2013, **13**, 16292.
- 2 K. L. Hong and L. J. Sooter, *BioMed Res. Int.*, 2015, **2015**, 31.
- 3 E. Torres-Chavolla and E. C. Alocilja, *Biosens. Bioelectron.*, 2009, **24**, 3175–3182.
- 4 M. Jarczewska, L. Kekedy-Nagy, J. S. Nielsen, R. Campos, J. Kjems, E. Malinowska and E. E. Ferapontova, *Analyst*, 2015, **140**, 3794–3802.
- 5 X. Wu, J. Chen, M. Wu and J. X. J. Zhao, *Theranostics*, 2015, **5**, 322–344.
- 6 H. Yoochan, L. Eugene, K. Minhee, S. Jin-Suck, Y. Dae Sung and Y. Jaemoon, *Nanotechnology*, 2016, **27**, 185103.
- 7 B. Deng, Y. Lin, C. Wang, F. Li, Z. Wang, H. Zhang, X.-F. Li and X. C. Le, *Anal. Chim. Acta*, 2014, **837**, 1–15.
- 8 Q. Wang, W. Liu, Y. Xing, X. Yang, K. Wang, R. Jiang, P. Wang and Q. Zhao, *Anal. Chem.*, 2014, **86**, 6572–6579.
- 9 J. Hwang, Y. Seo, Y. Jo, J. Son and J. Choi, *Sci. Rep.*, 2016, **6**, 34778.
- 10 M. McKeague, A. Foster, Y. Miguel, A. Giamberardino, C. Verdin, J. Y. S. Chan and M. C. DeRosa, *RSC Adv.*, 2013, **3**, 24415–24422.
- 11 X. Yang, Y. Wang, K. Wang, Q. Wang, P. Wang, M. Lin, N. Chen and Y. Tan, *RSC Adv.*, 2014, **4**, 30934–30937.
- 12 H.-J. Zhang, Y.-H. Lu, Y.-J. Long, Q.-L. Wang, X.-X. Huang, R. Zhu, X.-L. Wang, L.-P. Liang, P. Teng and H.-Z. Zheng, *Anal. Methods*, 2014, **6**, 2982–2987.
- 13 P. Zuo, X. Li, D. C. Dominguez and B.-C. Ye, *Lab Chip*, 2013, **13**, 3921–3928.
- 14 B. Jin, S. Wang, M. Lin, Y. Jin, S. Zhang, X. Cui, Y. Gong, A. Li, F. Xu and T. J. Lu, *Biosens. Bioelectron.*, 2017, **90**, 525–533.
- 15 D. Lu, L. He, G. Zhang, A. Lv, R. Wang, X. Zhang and W. Tan, *Nanophotonics*, 2017, **6**(1), 109–121.
- 16 R. E. Wang, Y. Zhang, J. Cai, W. Cai and T. Gao, *Curr. Med. Chem.*, 2011, **18**, 4175–4184.
- 17 N. Duan, H. Zhang, Y. Nie, S. Wu, T. Miao, J. Chen and Z. Wang, *Anal. Methods*, 2015, **7**, 5186–5192.
- 18 C. Meng, Z. Dai, W. Guo, Y. Chu and G. Chen, *Nanomater. Nanotechnol.*, 2016, **6**, 33.
- 19 B. Esteban-Fernández de Ávila, M. A. Lopez-Ramirez, D. F. Báez, A. Jodra, V. V. Singh, K. Kaufmann and J. Wang, *ACS Sens.*, 2016, **1**, 217–221.
- 20 L. Gao, Q. Li, R. Li, L. Yan, Y. Zhou, K. Chen and H. Shi, *Nanoscale*, 2015, **7**, 10903–10907.
- 21 N. Duan, W. Gong, Z. Wang and S. Wu, *Anal. Methods*, 2016, **8**, 1390–1395.
- 22 P. Singh, R. Gupta, M. Sinha, R. Kumar and V. Bhalla, *Microchim. Acta*, 2016, **183**, 1501–1506.
- 23 F. Melaine, C. Coilhac, Y. Roupioz and A. Buhot, *Nanoscale*, 2016, **8**, 16947–16954.
- 24 Q. Wang, J. Huang, X. Yang, K. Wang, L. He, X. Li and C. Xue, *Sens. Actuators, B*, 2011, **156**, 893–898.
- 25 E. Zeidan, R. Shivaji, V. C. Henrich and M. G. Sandros, *Sci. Rep.*, 2016, **6**, 26714.
- 26 O. A. Alsager, S. Kumar, B. Zhu, J. Travas-Sejdic, K. P. McNatty and J. M. Hodgkiss, *Anal. Chem.*, 2015, **87**, 4201–4209.
- 27 C.-C. Huang, Y.-F. Huang, Z. Cao, W. Tan and H.-T. Chang, *Anal. Chem.*, 2005, **77**, 5735–5741.
- 28 M. Bauch, S. Hageneder and J. Dostalek, *Opt. Express*, 2014, **22**, 32026–32038.
- 29 M. Bauch, K. Toma, M. Toma, Q. Zhang and J. Dostalek, *Plasmonics*, 2014, **9**, 781–799.
- 30 L.-Q. Chu, R. Förch and W. Knoll, *Angew. Chem., Int. Ed.*, 2007, **46**, 4944–4947.
- 31 F. Yu, B. Persson, S. Löfås and W. Knoll, *J. Am. Chem. Soc.*, 2004, **126**, 8902–8903.
- 32 Q. W. Song, M. S. Peng, L. Wang, D. C. He and J. Ouyang, *Biosens. Bioelectron.*, 2016, **77**, 237–241.
- 33 Y. F. Pang, Z. Rong, R. Xiao and S. Q. Wang, *Sci. Rep.*, 2015, **5**, 1.
- 34 D. A. Weitz, S. Garoff, C. D. Hanson, T. J. Gramila and J. I. Gersten, *J. Lumin.*, 1981, **24**, 83–86.
- 35 H. Cang, Y. Liu, Y. Wang, X. Yin and X. Zhang, *Nano Lett.*, 2013, **13**, 5949–5953.
- 36 M. E. Koivunen and R. L. Krogsrud, *Lab. Med.*, 2006, **37**, 490–497.
- 37 A. T. Csordas, A. Jørgensen, J. Wang, E. Gruber, Q. Gong, E. R. Bagley, M. A. Nakamoto, M. Eisenstein and H. T. Soh, *Anal. Chem.*, 2016, **88**, 10842–10847.
- 38 K.-A. Lee, J.-Y. Ahn, S.-H. Lee, S. Singh Sekhon, D.-G. Kim, J. Min and Y.-H. Kim, *Sci. Rep.*, 2015, **5**, 10897.
- 39 A. Sosic, A. Meneghello, E. Cretaio and B. Gatto, *Sensors*, 2011, **11**, 9426–9441.
- 40 A. Chen, M. Yan and S. Yang, *TrAC, Trends Anal. Chem.*, 2016, **80**, 581–593.
- 41 J. Liu, W. Bai, S. Niu, C. Zhu, S. Yang and A. Chen, *Sci. Rep.*, 2014, **4**, 7571.

- 42 J.-H. Park, J.-Y. Byun, W.-B. Shim, S. U. Kim and M.-G. Kim, *Biosens. Bioelectron.*, 2015, **73**, 26–31.
- 43 Y. Tang, F. Long, C. Gu, C. Wang, S. Han and M. He, *Anal. Chim. Acta*, 2016, **933**, 182–188.
- 44 H. Yu, J. Canoura, B. Guntupalli, X. Lou and Y. Xiao, *Chem. Sci.*, 2017, **8**, 131–141.
- 45 S. E. Lee, Q. Chen, R. Bhat, S. Petkiewicz, J. M. Smith, V. E. Ferry, A. L. Correia, A. P. Alivisatos and M. J. Bissell, *Nano Lett.*, 2015, **15**, 4564–4570.
- 46 C. Liu, X. Liu, Y. Qin, C. Deng and J. Xiang, *RSC Adv.*, 2016, **6**, 58469–58476.
- 47 N. Yildirim, F. Long, C. Gao, M. He, H.-C. Shi and A. Z. Gu, *Environ. Sci. Technol.*, 2012, **46**, 3288–3294.
- 48 Q. Zhou, T. Kwa, Y. Gao, Y. Liu, A. Rahimian and A. Revzin, *Lab Chip*, 2014, **14**, 276–279.
- 49 K. S. McKeating, A. Aube and J.-F. Masson, *Analyst*, 2016, **141**, 429–449.
- 50 S. Ohlson, C. Jungar, M. Strandh and C.-F. Mandenius, *Trends Biotechnol.*, 2000, **18**, 49–52.
- 51 M. Strandh, B. Persson, H. Roos and S. Ohlson, *J. Mol. Recognit.*, 1998, **11**, 188–190.
- 52 E. Meiby, S. Knapp, J. M. Elkins and S. Ohlson, *Anal. Bioanal. Chem.*, 2012, **404**, 2417–2425.
- 53 M.-D. Duong-Thi, E. Meiby, M. Bergström, T. Fex, R. Isaksson and S. Ohlson, *Anal. Biochem.*, 2011, **414**, 138–146.
- 54 L. J. Nielsen, L. F. Olsen and V. C. Ozalp, *ACS Nano*, 2010, **4**, 4361–4370.
- 55 F. Melaine, Y. Roupioz and A. Buhot, *Microarrays*, 2015, **4**, 41.
- 56 D. E. Huizenga and J. W. Szostak, *Biochemistry*, 1995, **34**, 656–665.
- 57 T. Liebermann and W. Knoll, *Colloids Surf., A*, 2000, **171**, 115–130.
- 58 K. E. Nelson, L. Gamble, L. S. Jung, M. S. Boeckl, E. Naeemi, S. L. Golledge, T. Sasaki, D. G. Castner, C. T. Campbell and P. S. Stayton, *Langmuir*, 2001, **17**, 2807–2816.
- 59 K. Sergelen, S. Fossati, A. Turupcu, C. Oostenbrink, B. Liedberg, W. Knoll and J. Dostalek, *ACS Sens.*, 2017, DOI: 10.1021/acssensors.7b00131.
- 60 T. Liebermann, W. Knoll, P. Sluka and R. Herrmann, *Colloids Surf., A*, 2000, **169**, 337–350.
- 61 A. Dasgupta, in *Therapeutic Drug Monitoring*, Academic Press, Boston, 2012, pp. 1–29, DOI: 10.1016/B978-0-12-385467-4.00001-4.
- 62 M. Luke, in *Therapeutic Drug Monitoring*, Academic Press, Boston, 2012, pp. 243–267, DOI: 10.1016/B978-0-12-385467-4.00012-9.
- 63 S. S. Zhao, N. Bukar, J. L. Toulouse, D. Pelechacz, R. Robitaille, J. N. Pelletier and J.-F. Masson, *Biosens. Bioelectron.*, 2015, **64**, 664–670.
- 64 B. S. Ferguson, D. A. Hoggarth, D. Maliniak, K. Ploense, R. J. White, N. Woodward, K. Hsieh, A. J. Bonham, M. Eisenstein, T. Kippin, K. W. Plaxco and H. T. Soh, *Sci. Transl. Med.*, 2013, **5**, 213ra165–213ra165.
- 65 M. Farias, M. W. Gorman, M. V. Savage and E. O. Feigl, *Am. J. Physiol.: Heart Circ. Physiol.*, 2005, **288**, H1586–H1590.
- 66 B. B. Fredholm, *Sleep Biol. Rhythms*, 2011, **9**, 24–28.
- 67 F. M. Gribble, G. Loussouarn, S. J. Tucker, C. Zhao, C. G. Nichols and F. M. Ashcroft, *J. Biol. Chem.*, 2000, **275**, 30046–30049.
- 68 Z. Liu, S. Chen, B. Liu, J. Wu, Y. Zhou, L. He, J. Ding and J. Liu, *Anal. Chem.*, 2014, **86**, 12229–12235.
- 69 M. Bauch and J. Dostalek, *Opt. Express*, 2013, **21**, 20470–20483.
- 70 Y. Wang, J. Dostálek and W. Knoll, *Biosens. Bioelectron.*, 2009, **24**, 2264–2267.
- 71 F. Saint-Marcoux, in *Therapeutic Drug Monitoring*, Academic Press, Boston, 2012, pp. 103–119, DOI: 10.1016/B978-0-12-385467-4.00005-1.